中國機械工程學刊第四十一卷第二期第 229~238 頁(民國一百零九年)
Journal of the Chinese Society of Mechanical Engineers, Vol.41, No.2, pp 229~238 (2020)

Ride Analysis of Track-Vehicle-Human Body Interaction Subjected to Random Excitation

Sono Bhardawaj*, Rakesh Chandmal Sharma* and Sunil Kumar Sharma**

Keywords：power spectral density, ride comfort, track recording car, lagrange's method

ABSTRACT

This paper considers a track-vehicle-human body 54 degrees of freedom (DoF) system formulated using Lagrange's method out of which 4 DoF to track system, 40 DoF to rail vehicle system and 10 DoF to lumped parameter bio-dynamic human body system are assigned. Stationary random track irregularities are measured with Track Recording Car and represented by Power Spectral Density functions using Fast Fourier Transformation. The formulated model is validated by comparing the results of accelerations analysis with the same determined through experimental measurements. The vehicle ride comfort is determined at the passenger seat based on standards specified in annexure ISO 2631-1. The vertical seat to head and vertical back support to head transmissibility of the human body model in seated backrest position is evaluated and validated through past reported studies.

INTRODUCTION

A rail vehicle is a complex dynamic system, and in its complete model, it consists of wheelaxles, carbody and bogie frame etc. which may be modelled as rigid (Zheng et al., 2015) or flexible (Zhou et al., 2009). The vehicle mass is supported by suspension elements i.e. springs and dampers which can be modelled as linear (Zhai et al. 1996; 2009), non-linear (Durali and Shahmehri, 2003; Sharma and Kumar, 2017) or piecewise linear.

Each element of the track and vehicle system may be modelled with a maximum six DoF plus additional DoF describing the component's elastic distortion (Wickens, 2003). In the latter case, these additional DoF may describe a Finite Element (FE) model of a structure or a series of natural modes of vibration. The track may be modelled as a continuous or discrete (Kargarnovin et al. 2005), beam or structure (Sadeghi and Askarinejad, 2010), single or two or even more layered system (Zakeri and Ghorbani, 2011) incorporating rail, rail pad, sleeper, fasteners, ballast, soil and subgrade. The dynamics of vehicle and track mainly depend on the wheel-rail interface where the interaction is a function of relative motion.

The human body is a dynamic system where inertial; elastic and dissipative properties change according to posture and from one person to another (Liang and Chiang, 2006). Human body parts are sensitive to whole-body vibration subjected to low-frequency excitation (Carlbom and Berg, 2002). In the past research, several mathematical models have been formulated based on diverse field measurements to describe the biodynamic characteristics of human body (Liang and Chiang, 2006). These models are lumped parameter, finite elements and multibody models. In a lumped-parameter system, the human body is modelled as multiple concentrated masses interconnected by springs and dampers. The FE model considers that the human body consists of several finite elements whose characteristics are determined through experiments on human corpses. Multibody human model considers multiple rigid bodies as kinematic links jointed by pin to form a planar mechanism or ball and socket joints to form a three-dimensional mechanism.

In this paper, the analysis consists of a 54 DoF track-vehicle-human body system formulated using Lagrange's method out of which 4 DoF to track system, 40 DoF to rail vehicle system and 10 DoF to lumped parameter model of the human body are assigned. The rail vehicle considered in the present analysis is Indian Railway Integral Coach Factory coach. The vehicle ride comfort is determined at the passenger seat based on standards laid in annexure ISO 2631-1 (ISO 2631-1, 1997) and the analysis is extended further for Vertical Seat To Head (VSTH) and Vertical Back support To Head (VBTH) transmissibility analysis with the biodynamic human body model.

MATHEMATICAL MODELLING OF HUMAN BODY-VEHICLE-TRACK SYSTEM

Paper Received May, 2019. Revised September, 2019. Accepted October, 2019. Author for Correspondence: Rakesh Chandmal Sharma and Sunil Kumar Sharma

* *Mechanical EngineeringDepartment, Maharishi Markandeshwar (Deemed to be University), Mullana, Ambala, India.*

** *Department of Mechanical Engineering, Amity School of Engineering and Technology, Amity University Uttar Pradesh, Noida, India*

Mathematical modelling of the human body

The human body (Fig. 1) is modelled to be seated in backrest posture with its head towards the direction of motion of the vehicle. It is divided into five parts i.e. head & neck, upper torso, viscera, pelvic and leg. Vertical and longitudinal motion is assigned to each part. The parameter values of the human body model are listed in Table 1.

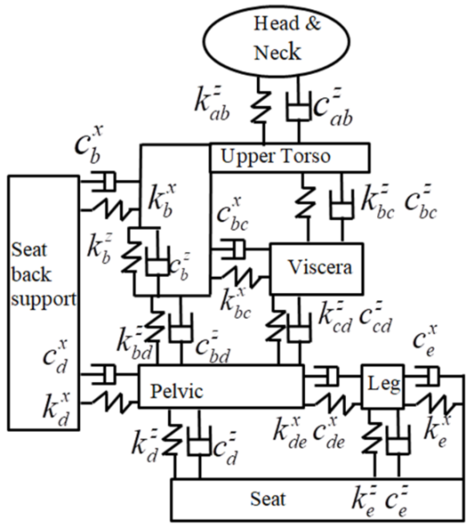

Fig. 1. Human body model in seated backrest posture.

Table 1. Human body parameters and their values.

Parameter	Value	Parameter	Value	Parameter	Value	Parameter	Value
m_a	6 kg	k_d^z	150 kN/m	k_{de}^x	2.25 kN/m	k_{bc}^x	24 kN/m
m_b	20 kg	k_e^x	0.016 kN/m	c_{de}^x	65 N-sec/m	c_{cd}^z	4.5×10^3 N-sec/m
m_c	13 kg	k_e^z	15 kN/m	c_e^z	100 N-sec/m	c_{bd}^z	850 N-sec/m
m_d	11 kg	c_b^x	160 N-sec/m	k_{cd}^z	170 kN/m	c_{bc}^z	14×10^3 N-sec/m
m_e	15 kg	c_b^z	340 N-sec/m	k_{bd}^z	7.5 kN/m	c_{ab}^z	140 N-sec/m
k_b^x	2.2 kN/m	c_d^x	16 N-sec/m	k_{bc}^z	750 kN/m		
k_b^z	16.2 kN/m	c_d^z	50 N-sec/m	k_{ab}^z	5 kN/m		
k_d^x	0.88 kN/m	c_e^x	15 N-sec/m	c_{bc}^x	275 N-sec/m		

Mathematical modelling of vehicle system

The vehicle model (Fig. 2) is formulated by considering rigid bodies i.e. seat back support, seat, carbody, bolster, bogie frame and wheelaxle. Single DoF assigned to seat back support i.e. vertical, two DoF assigned to seat i.e. vertical and lateral, five DoF assigned to carbody and each bogie frame i.e. vertical, lateral, roll, pitch and yaw, three DoF assigned to each bolster i.e. vertical, lateral and roll, four DoF assigned to each wheelaxle i.e. vertical, lateral, roll and yaw. The vehicle parameters (mass, inertial, geometric and seat) and their values are listed in Table 2. The vehicle suspension parameters in the present analysis are considered as linear and piecewise linear; their characteristics and parameter values are described in Table 3.

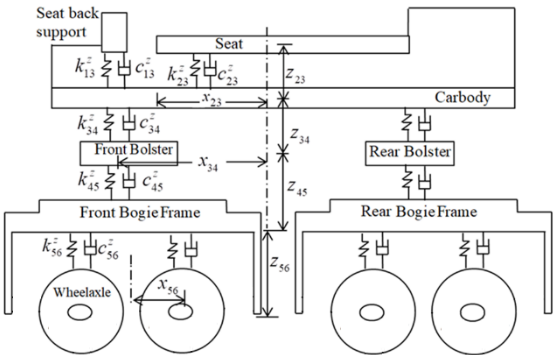

Fig. 2. Vehicle model.

Table 2. Vehicle parameters (mass, inertial, geometric and seat) and their values.

Parameter	Value	Parameter	Value	Parameter	Value
m_1	16 kg	I_4^y	00	k_{23}^z	25.5×10^{-3} MN/m
m_2	16 kg	I_4^z	336.4 kg-m^2	c_{23}^z	1.04×10^{-3} MN-s/m
m_3	33740 kg	I_5^x	1713 kg-m^2	z_{23}	0.5 m
m_4	400 kg	I_5^y	3206 kg-m^2	x_{23}	7.2915 m
m_5	2600 kg	I_5^z	4763 kg-m^2	z_{34}	1.286 m
m_6	1600 kg	I_6^x	1271 kg-m^2	x_{34}	7.3915 m
I_3^x	56932 kg-m^2	I_6^y	117 kg-m^2	z_{45}	m
I_3^y	1307220 kg-m^2	I_6^z	1271 kg-m^2	z_{56}	0.209 m
I_3^z	1309744 kg-m^2	k_{13}^z	25×10^{-3} MN/m	x_{56}	1.448 m
I_4^x	307 kg-m^2	c_{13}^z	1×10^{-3} MN-s/m		

Table 3. Vehicle suspension parameters; their characteristics and values.

Parameter	Suspension characteristics	Spring force (MN)	Displacement (m)	Damping force (MN)	Velocity (m/s)
k_{34}^z	Linear	35	1	-	-

c^z_{34}	Linear	-	-	0.0311	1
k^z_{45}	Piecewise Linear	-0.1087	-0.1156	-	-
		-35.1087	-1.1156	-	-
c^z_{45}	Linear	-	-	0.0589	1
k^z_{56}	Piecewise Linear	-0.05931	-0.1121	-	-
		-17.559	-1.1121	-	-
c^z_{56}	Linear	-	-	-0.0412	-1

Mathematical modelling of track

Track is modelled as a two-layer continuous system with rail and sleeper as rigid bodies (Fig. 3). The rail pad properties are lumped together with sleeper. The rail-sleeper properties per unit length and soil properties per square meter area per wheel are considered in the analysis. Track and sleeper stiffness and track damping per square meter area per wheel is incorporated in the analysis. The rail surface is assigned three DoF i.e. vertical, lateral & pitch and the sleeper is assigned single DoF i.e. vertical. The parameter values of the track model are listed in Table 4.

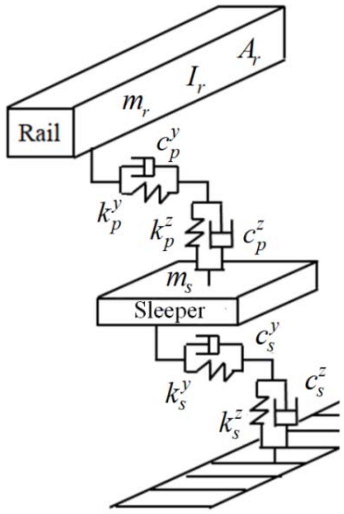

Fig. 3. Track model.

Table 4. Track parameters and their values.

Parameter	Value	Parameter	Value	Parameter	Value
m_r	56 kg	k_p^z	220 MN/m	k_s^z	90 MN/m
m_s	110 kg	c_p^z	0.098 MN-s/m	c_s^z	0.040 MN-s/m
I_r	3.217×10^{-5} m^4	k_p^y	280 MN/m	k_s^y	78 MN/m
A_r	7.77×10^{-3} m^2	c_p^y	0.058 MN-s/m	c_s^y	0.080 MN-s/m

Measurement and modelling of track inputs

The tangent track irregularities (Garg and Dukkipati, 1984) are normally defined by the following four geometrical parameters i.e. alignment, gauge, cross-level and unevenness of left & right rails as shown in Fig. 4.

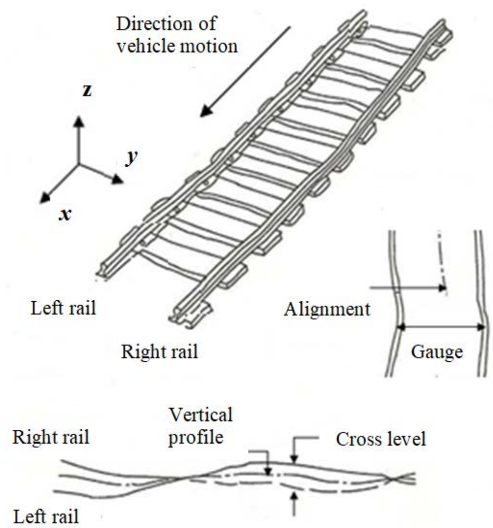

Fig. 4. Definitions of track irregularity parameters (Garg and Dukkipati, 1984).

The track has small imperfections in material and tolerances, manufacturing errors in the track components, terrain irregularities and survey errors during the design & construction of the track. The progressive deterioration of track geometry also occurs due to traffic and environmental factors. The track geometry variations which largely affect the rail vehicle behaviour are measured by Track Recording Car (TRC) using either the chord offset principle or inertial principle. The track profile of a wavelength ranging between 0.1 to 100 m is of prime interest for track designers. Since track profiles are random, these are better described by statistical techniques. The variations in track geometry parameters are random in nature. The parameters are measured by appropriate transducers in TRC by research wing of Indian Railways, Research Designs Standards Organisation, Lucknow (India) and sampled at a distance of 0.404 m. The signals obtained from the transducers are further processed by hardware signal conditioners and analyzed by the software inbuilt within the TRC.

The sample output obtained from the TRC is shown in Table 5. In Table 5 Abbreviations UNL is Unevenness of left rail, UNR is Unevenness of right rail, XL is Cross-level, ALL is Alignment left, ALR is

Alignment right, G is Gauge, CAV is Coach Acceleration Vertical, CAL is Coach Acceleration Lateral, TW is Twist, V is Speed, GF is Ground Feature.

Table 5. Rail profile parameters obtained from TRC.

TGMS-10 VERSION 1.40, RAW DATA PROFILES										
UNL× 4	UNR × 4	XL× 4	ALL× 4	ALR × 4	G× 4	CAV	CAL	TW × 4	V	GF
36	-13	-46	6	7	12	40	0	-32	21306	0
37	-9	-42	9	6	14	42	-42	-34	18505	0
37	-6	-41	10	8	16	12	-46	-33	19309	0
38	-3	-38	8	5	15	13	-32	-28	18395	0
32	0	-36	6	6	14	14	-22	-28	21043	0

The track irregularities at a future instant of time cannot be predicted and therefore are classified as random. If the surface profile is obtained, its frequency analysis may be performed to estimate the amplitude for the various wavelengths present. In random vibrations, the mean square value of the amplitude is of prime interest instead of the value of the amplitude, as it is related to average energy.

A harmonic component $Z_n(x)$ with amplitude Z_n and wavelength l_{wn} can be expressed as:

$$Z_n(x) = Z_n \sin(2\pi x / l_{wn}) = Z_n \sin \Omega_n x \tag{1}$$

Meanwhile, Ω_n is the spatial frequency (rad/m) of the harmonic component. The mean square value of the component $Z_n(x)$ is expressed as:

$$\bar{Z}_n^2 = \frac{1}{l_{wn}} \int_0^{l_{wn}} \left[Z_n \sin\left(\frac{2\pi x}{l_{wn}}\right)\right]^2 dx = Z_n^2 / 2 \tag{2}$$

A random function consists of a large number of frequencies and mean square values can be plotted as a continuous function. Substituting $S(n\Omega_0)$ as the density of the mean square value in the interval $\Delta\Omega$ at the frequency $n\Omega_0$, the discrete spectral density may be expressed as:

$$S(n\Omega_0) = \frac{Z_n^2}{2\Delta\Omega} = \frac{\bar{Z}_n^2}{\Delta\Omega} \tag{3}$$

For a continuous function, the Power Spectral Density (PSD) of a random process provides the frequency composition of the data in terms of the spectral density of its mean square value. The mean square value of the sample time history record, in a frequency range Ω to $\Omega + \Delta\Omega$, is obtained by passing the sample record through a band-pass filter with sharp cutoff features and computing the average of the squared output from the filter. PSD function is expressed as:

$$S_z(\Omega) = \lim_{T\to\infty} \lim_{\Delta\Omega\to\infty} \frac{1}{\Delta\Omega} \frac{1}{T} \int_0^T Z_F^2 dt \tag{4}$$

Meanwhile, Z_F is band-pass filtered output of Z_n and Ω is spatial frequency (cycles/m).

The signals of interest for track geometry parameters are in the frequency range of 0.01 cycles/m to 10 cycles/m. Since the signals are sampled at a distance of 0.404 m, the maximum frequency which could be analyzed is 1/(2×0.404) cycles/m. In other words, the wavelength less than 0.808 m cannot be measured and analyzed. The Fast Fourier Transform (FFT) algorithm used for computing discrete Fourier Transform requires the number of samples to be an integral power of 2. Since the minimum track length to be analyzed was around 200 m, a minimum of 512 data points have been selected for FFT analysis and subsequently for PSD estimation. The selection of 512 data points gives sampled track length of 206.8 m. However, any multiple of 512 data points may be selected for analysis depending on the capacity of the computer. The total frequency spectrum of 0.01 cycle/m to 10 cycles/m has been divided into 256 segments. Thus each frequency interval is of 0.039 cycles/m, which is acceptable.

The software in the FFT analysis uses a square window called flat-topped window. It will be desirable to obtain the smallest variance from a fixed amount of computation, regardless of the number of data points used. Two possible situations arise in data recording and analysis. In the first case when the data are recorded in real-time, the data reduction is computer limited. In this situation, the data are segmented without any overlapping. The first 2M data points constitute segment number 1; the next 2M data points constitute segment number 2; and so on, up to segment number K, for a total of 2KM data points. The variance in this case, relative to a single segment, is reduced by a factor K/2.

In the second case, when the data are already recorded and analyzed, it is desired that the smallest variance from a fixed number of available data points is obtained. In this situation smallest spectral variance per data points is optimal, to overlap the segments by one half of their length. The first and second sets of M points are segment 1; the second and third sets of M points are segment 2; and so on, up to segment number K, which is made of the Kth and (K+1)th sets of M points. The total number of sampled points are, therefore (K+1) M, just over half as many as with non-overlapping segments. The reduction in variance is reduced by a factor of about 9K/11. This is, however, significantly better than the reduction of about K/2 that would have resulted if the number of data points were segmented without overlapping. The flow chart for the PSD software is shown in Fig. 5.

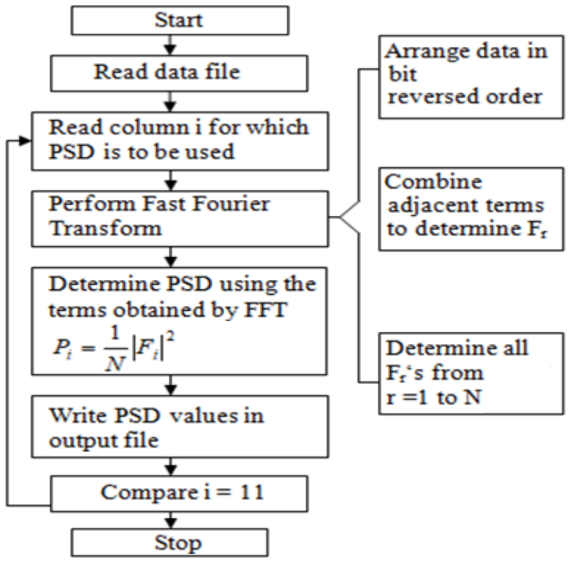

Fig. 5. Flowchart for PSD Software.

PSD function of irregularity of track surface as a function of spatial frequency Ω is expressed as:

$$P_r(\Omega)=C\,\Omega^{nT} \quad (5)$$

Meanwhile, C is a constant, n is the slope of amplitude with frequency Ω, T is time lag between different wheels. From the measurements using TRC, different values of C and n are obtained through simulations and considered as inputs in the present analysis are listed in Table 6.

Table 6. PSD of Track Inputs.

PSD input (mm^2/cycle/meter)	C	n
Auto-PSD function of vertical unevenness of track surface	0.0946	-2.1271
Cross-PSD function of vertical unevenness between the left and right rail	0.0246	-2.3726
Auto-PSD function of lateral irregularity of track surface	0.0546	-2.2576
Cross-PSD function of lateral irregularity between the left and right rail	0.278	-2.2982

EQUATIONS OF MOTION AND COMPLEX FREQUENCY RESPONSE FUNCTION

The equations of motion are obtained using the Lagrange's method and may be expressed as:

$$\frac{d}{dt}\left[\frac{\partial L}{\partial \dot{q}_i}\right]-\frac{\partial L}{\partial q_i}+\frac{\partial E_P}{\partial q_i}+\frac{\partial E_D}{\partial \dot{q}_i}=Q_i \quad (6)$$

Meanwhile, L is Largrangian operator, E_P is spring energy of the system, E_d is Rayliegh's dissipation function, Q_i is generalized force and q_i is independent generalized coordinate. When the vehicle is moving on a straight-line track, wheel-track interactive forces are the function of law of creep and dynamic behaviour of the whole system and general equation of motion is expressed as.

$$[M](\ddot{y}_i)+[C](\dot{y}_i)+[K](y_i)=\varphi(x,\dot{x})+\varphi(y,\dot{y},\ddot{y}) \quad (7)$$

In Eq. (7) $\phi(x,\dot{x})$ and $\phi(y,\dot{y},\ddot{y})$ are the constraint forces offered by track due to creep and the track input function respectively. In the present analysis linear creepage at rail-wheel interaction is considered and creep coefficients proposed in Kalker's linear creep theory (Kalker, 1979) have been used. To derive complex frequency response function, harmonic input is provided at one wheel at an instant and the inputs at the remaining wheels are kept zero during that period. Input function is expressed as:

$$q_r=Q_r\,e^{i\omega t} \quad (8)$$

r = 1, 2,…….8.

The response function of the system can be expressed as:

$$y_i=Y_i\,e^{i\omega t} \quad (9)$$

Meanwhile, Q_r and Y_i are the amplitude of input and response function respectively. Eq. (7) may be expressed in the form as:

$$([M](-\omega^2)+[C](i\omega)+[K])y_i\,e^{i\omega t}=[F_r(\omega)]q_r\,e^{i\omega t} \quad (10)$$

$$[D_1]H_r(\omega)=F_r(\omega) \quad (11)$$

Meanwhile, $[F_r(\omega)]$ is the force matrix, D_1 is the dynamic stiffness matrix and $H_r(\omega)=(y_i/q_r)$ is the complex frequency response function for r$^{\text{th}}$ input, ω is angular frequency (rad/s).

ANALYSIS OF RIDE BEHAVIOR

If $\ddot{z}_3$ and $\ddot{y}_3$ are the vertical and lateral acceleration of carbody mass centre, the vertical and lateral acceleration at seat i.e. $\ddot{z}_2$ and $\ddot{y}_2$ respectively may be expressed as:

$$\ddot{z}_2=\ddot{z}_3+x_{23}\ddot{\varphi}_3+z_{23}\ddot{\theta}_3 \quad (12)$$

$$\ddot{y}_2=\ddot{y}_3+x_{23}\ddot{\psi}_3+z_{23}\ddot{\theta}_3 \quad (13)$$

Meanwhile, $\ddot{\theta}_3,\ddot{\varphi}_3$ and $\ddot{\psi}_3$ are roll, pitch and yaw acceleration of carbody mass centre respectively. For systems excited by random inputs, the input-output relation of PSD is expressed as:

$$[P_{yy}(\omega)]\;=[H_r(\omega)]\;\;[P_r(\omega)]\;\;[H_r(\omega)]^T \quad (14)$$

The Mean Square Acceleration Response (MSAR) at the seat in the vertical and lateral direction is expressed as:

$$P_{yy}(f)=(2\pi f)^4\,[H_r(\omega)]\,[P_r(\omega)]\;\;[H_r(\omega)]^T \quad (15)$$

Root Mean Square Acceleration Response (RMSAR) at a central frequency f_o is obtained through integrating the PSD function in one third octave band and is expressed as:

$$a_i = sqrt[(2\pi)^4 \int_{0.89\,fo}^{1.12\,fo} [P_{yy}(f)](f)^4 df] \quad (16)$$

In the present analysis a_i is evaluated in vertical and lateral direction and represented as a_{iz} and a_{iy} respectively.

VALIDATION OF MATHEMATICAL MODEL

The present model is validated by comparing MSAR (PSD acceleration) at the seat in vertical and lateral direction obtained through analysis with the same obtained through experimental measurements that are obtained from Research Designs Standards Organisation, Lucknow, INDIA. The rail vehicle is travelled with a constant speed of 100 km/hr on a straight track.

The measurements are processed in two steps. In the initial step, the accelerations are recorded for 2 Km straight specimen run-down track and this record is validated by covering a long run of about 25 Km in the next step. A strain gauge accelerometer (Range: ±1 g and ±2 g; Frequency response: 25 Hz; Excitation: 5V AC/DC; Sensitivity: 360 mV/V/g; Damping: silicon fluid) is kept at the seat inside the carbody. The vertical and lateral MSAR curve obtained from simulation (Fig. 6 and 7) and experimental measurements (Fig. 8 and 9) found to be good agreement and therefore the present model is validated.

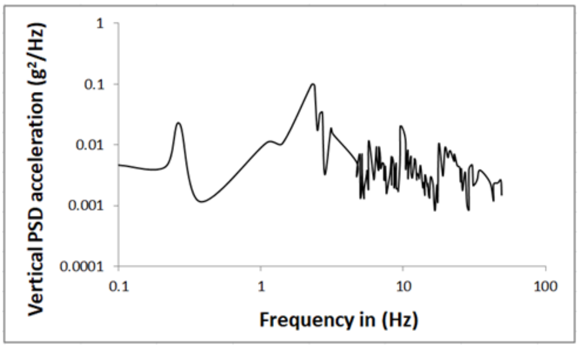

Fig. 6. Vertical PSD acceleration at the seat (simulation).

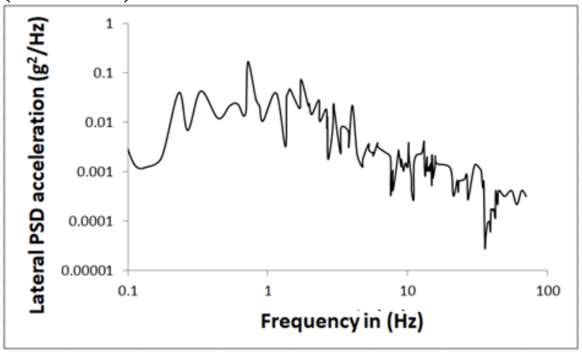

Fig. 7. Lateral PSD acceleration at the seat (simulation).

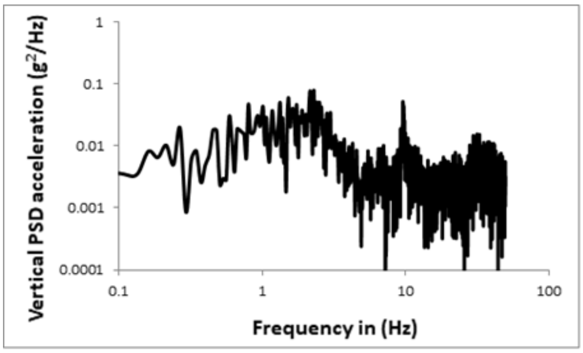

Fig. 8. Vertical PSD acceleration at the seat (experimental measurements).

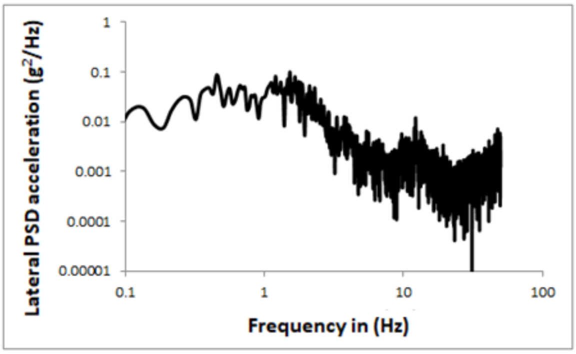

Fig. 9. Lateral PSD acceleration at the seat (experimental measurements).

RIDE COMFORT EVALUATION

ISO 2631-1 ride comfort standards are the most universally accepted criteria for the evaluation of ride quality indices. Different time limits of exposure are established in this standard which is termed as ISO 2631-1 comfort boundaries. The acceleration pattern must remain inside these boundaries to achieve comfort level for respective time exposure. Distinct criteria are used for vertical and lateral accelerations. The roll and yaw acceleration influence the lateral acceleration and pitch and roll acceleration influence the vertical acceleration for the points of acceleration considered in this analysis.

When the vehicle vibration environment is a broadband, i.e. has frequency content over a wide range, the recommended procedure is to compute the RMSAR in 1/3 octave frequency band. As the influence of the acceleration on human body differs at different frequencies, the comfort boundaries were formed through a large number of analyses through different transport agencies. The principal frequency weighting values described in ISO 2631-1 are multiplied in RMSAR and the weighted Root Mean Square (RMS) acceleration values are plotted for frequency (Fig. 10 and 11).

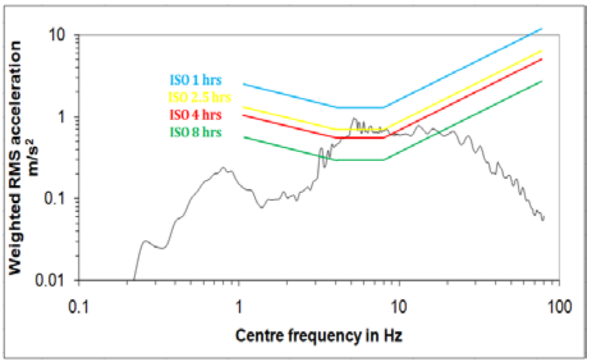

Fig. 10. Vertical weighted RMS acceleration at the seat (simulation).

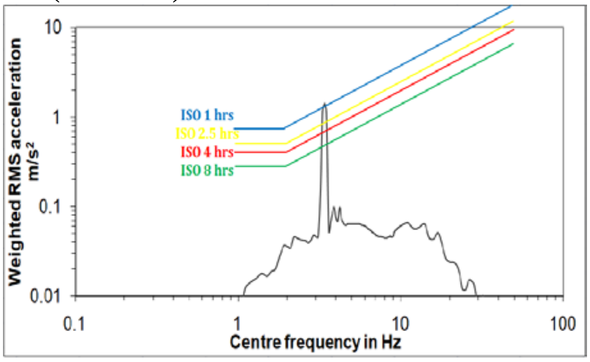

Fig. 11. Lateral weighted RMS acceleration at the seat (simulation).

ISO 2631-1 considers RMS acceleration as the basic measure of vibration evaluation. As per its guidelines the value of overall weighted acceleration in vertical directions is expressed as:

$$a_{Wz} = [\sum W_k a_{iz})^2]^{1/2} \quad (17)$$

and the value of overall weighted acceleration in lateral directions is expressed as:

$$a_{Wy} = [\sum W_d a_{iy})^2]^{1/2} \quad (18)$$

Meanwhile, W_k and W_d are the principal frequency weightings in vertical and lateral directions respectively.

The vibration total value of weighted RMS acceleration as per annexure ISO 2631-1 is expressed as:

$$a_v = [k_y^2 a_{Wy}^2 + k_z^2 a_{Wz}^2]^{1/2} \quad (19)$$

Meanwhile, k_y and k_z are the multiplying factors in lateral and vertical direction respectively and their values specified in annexure ISO 2631-1 are 1.4 and 1 respectively.

VERTICAL SEAT TO HEAD AND VERTICAL BACK SEAT TO HEAD TRANSMISSIBILITY ANALYSIS

The analysis of human response, when subjected to vibration in sitting posture, is related to mode of transportation where the passenger is exposed to whole-body vibration. The crucial aspects in this context are the vibration characteristic of seat, vibration environment and human body vibrational response. A human body may be modelled in different ways during train travel. In seated posture, it may be modelled in several ways e.g. erect without backrest, with backrest, forward-leaning on table and erected with leg fold. A particular model may not consider all the factors but may describe the aspect of the system.

The objective of this analysis is to study the human body response under vertical excitation under the stated frequency range. In this study vertical response at seat and back seat support obtained through simulation is taken as the input to determine VSTH and VBTH transmissibility in seated backrest position. The transmissibility analysis is restricted to a frequency range from 1 to 20 Hz as the eigenvalues of human body parts and resonating frequencies remain in this zone. VSTH transmissibility of the considered model is expressed as:

$$Tr_{VSTH}(f) = \frac{z_a(f)}{z_2(f)} \quad (20)$$

$z_2(f)$ is the vertical input response at the seat as a function of temporal frequency and $z_a(f)$ is human head and neck vertical output response.

VBTH transmissibility of the considered model is expressed as:

$$Tr_{VBTH}(f) = \frac{z_a(f)}{z_1(f)} \quad (21)$$

$z_1(f)$ is the vertical input response at the seat back support as a function of temporal frequency.

The results of VSTH and VBTH transmissibility obtained from the present analysis are validated by comparing the curve obtained in Fig. 12 and 13 with curves of mean Seat to Head Transmissibility (STHT) characteristics (Fig. 14) obtained in different reported studies (Paddan and Griffin 1988; Wang et al., 2006). The STHT characteristics obtained from past research reflect significant variations which are attributed to differences in factors i.e. measurement & analysis methods, experiment designs, subject anthropometry and nature of whole-body vibration. Peak transmissibility values in seating position with erect and forward lean postures are higher than the same obtained in seating backrest posture. From the majority of past research, peak transmissibility value is obtained as 1.5-2.5 and is observed in the frequency range of 3-8 Hz (Fig. 14). Therefore the results of VSTH and VBTH transmissibility of present analysis appear to be in good agreement with past reported research.

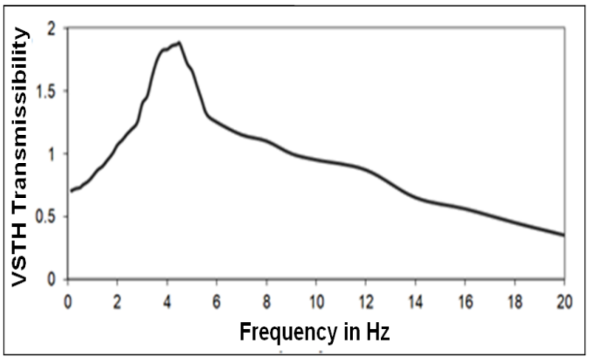

Fig. 12. VSTH Transmissibility.

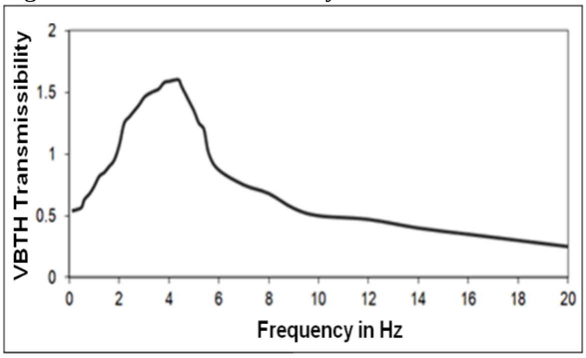

Fig. 13. VBTH Transmissibility.

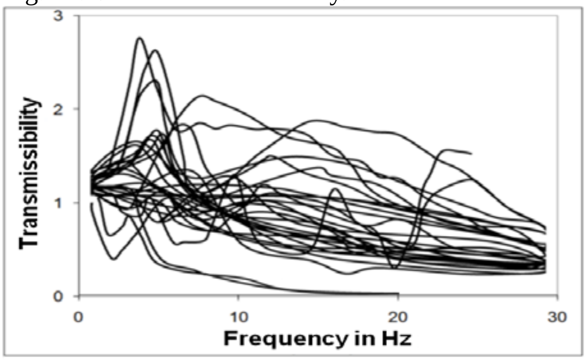

Fig. 14. Variations in mean STHT characteristics (synthesized data) obtained from different past research (Paddan and Griffin 1988; Wang et al., 2006).

NUMERICAL RESULTS

The simulation in the present study is made in MATLAB environment. MATLAB provides the solution to eigenvalue, stability and ride comfort analysis of a dynamic system with ease once the equations of motion are developed. The rail vehicle is considered to be running at 100 km/hr on straight-line track subjected to random irregularities. As the human body is modelled as a single mass travelling in seated posture, the ride comfort is studied for the exposure time of 1, 2.5, 4 and 8 hours.

The weighted vertical RMS acceleration curve (Fig. 10) is found to be within 1 hour comfort boundary specified for ISO vertical ride comfort. The weighted vertical RMS acceleration curve lies outside 2.5 hours ISO comfort boundary for frequencies nearly from 5 Hz to 6.5 Hz and at 8 Hz, lie outside 4 hours ISO comfort boundary for frequencies nearly from 4 Hz to 9 Hz and lie outside 8 hours ISO comfort boundary for frequencies nearly from 3 Hz to 18 Hz. The weighted lateral RMS acceleration curve (Fig. 11) is found to be within comfort boundary except for frequency nearly from 3.25 to 3.5 Hz for all exposure time considered in the analysis from 1 hr to 8 hr. As the natural frequencies of different parts lie within 15 Hz, therefore it can be concluded that Indian Railway Integral Coach Factory coach is not suitable for 8 hrs travel in seated posture. The vertical ride is more crucial as compared to lateral ride as the lateral ride is found to be in discomfort zone at a narrow frequency range nearly 3.5 Hz regardless of exposure time.

The overall weighted vertical RMS acceleration and overall weighted lateral RMS acceleration for the frequency range from 1 to 80 Hz are determined as 1.24 m/s^2 and 0.6 m/s^2 respectively. The total value of weighted RMS acceleration is determined as 1.49 m/s^2 which suggests that ride comfort index of Indian Railway Integral Coach Factory coach lies in category ‘uncomfortable’ as per ISO 2631-1 specifications.

Fig. 12 depicted that VSTH transmissibility are critical from the frequency range from 2 to 6 Hz and peak transmissibility is observed at a frequency of nearly 4.5 Hz. Fig. 13 revealed that average value of VBTH transmissibility at different frequencies are lower as compared to VSTH transmissibility in the frequency range of study, peak VBTH transmissibility is observed at a frequency of nearly 4.3 Hz. The results of VSTH and VBTH transmissibility predict that the human body models describe the best representation of biodynamic response study under backrest seated posture subjected to whole-body vibration.

REFERENCES

Carlbom, P. and Berg, M., “Passengers, seats and carbody in rail vehicle dynamics,” Vehicle System Dynamics, Vol. 37, pp. 290-300(2002).

Durali, M. and Shahmehri, B., “Nonlinear analysis of train derailment in severe braking,” J. of Dyn. Systems, Measurement and Control, Trans. of the ASME, Vol. 125, pp. 48-53(2003).

Garg, V.K. and Dukkipati Rao, V., “Dynamics of railway vehicle systems,” Academic Press, New York, (1984).

Goswami, B., Rathi, A., Sayeed, S., Das, P., Sharma, R.C., Sharma, S.K., Optimization Design for Aerodynamic Elements of Indian Locomotive of Passenger Train. In: Advances in Engineering Design. Lecture Notes in Mechanical Engineering. Springer, Singapore pp. 663–673. (2019)

ISO-2631, “Mechanical vibration and shock evaluation of human exposure to whole body vibrations- part 1,” general requirements, (1997).

Kalker, J.J., “Survey of wheel-rail rolling contact theory,” Vehicle System Dynamics, Vol. 5, pp. 317-358(1979).

Kargarnovin, M.H., Younesian, D., Thompson, D., and Jones, C., "Ride comfort of high- speed trains traveling over railway bridges," Vehicle System Dynamics, Vol. 43, No. 3, pp. 173-199(2005).

Liang, C-C. and Chiang, C-F., "A study on biodynamic models of seated human subjects exposed to vertical vibration," International Journal of Industrial Ergonomics, Vol. 36, No. 10, pp. 869-890(2006).

Paddan, G.S. and Griffin, M.J., "The transmission of translational seat vibration to the head-I. Vertical seat vibration," Journal of Biomechanics, Vol. 21, pp. 191-197(1988).

Palli, S., Koona, R., Sharma, S.K., Sharma, R.C., A Review on Dynamic Analysis of Rail Vehicle Coach. Int. J. Veh. Struct. Syst. Vol. 10, pp. 204–211 (2018). https://doi.org/10.4273/ijvss.10.3.10

Sadeghi, J. and Askarinejad, H., "Development of improved railway track degradation models," Structure and Infrastructure Engineering, Vol. 6, No. 6, pp. 675–688(2010).

Sharma, S.K. and Kumar, A., "Impact of electric locomotive traction of the passenger vehicle ride quality in longitudinal train dynamics in the context of Indian railways," Mechanics & Industry, Vol. 18, No. 2, pp. 222(2017).

Sharma, R.C., Palli, S., Sharma, S.K., Roy, M., Modernization of railway track with composite sleepers. Int. J. Veh. Struct. Syst. Vol. 9, pp.321–329 (2017). https://doi.org/10.4273/ijvss.9.5.10

Sharma, R.C., Sharma, S.K., Sensitivity analysis of three-wheel vehicle's suspension parameters influencing ride behavior. Noise Vib. Worldw. Vol. 49, No.7-8, pp. 272–280 (2018) https://doi.org/10.1177/0957456518796846

Sharma, S.K., Multibody analysis of longitudinal train dynamics on the passenger ride performance due to brake application. Proc. Inst. Mech. Eng. Part K J. Multi-body Dyn. Vol. 233, No.2, pp. 266–279 (2019). https://doi.org/10.1177/1464419318788775

Sharma, S.K., Kumar, A., Impact of Longitudinal Train Dynamics on Train Operations: A Simulation-Based Study. J. Vib. Eng. Technol. Vol. 6, No.3, pp.197–203 (2018). https://doi.org/10.1007/s42417-018-0033-4

Sharma, S.K., Saini, U., Kumar, A., Semi-active Control to Reduce Lateral Vibration of Passenger Rail Vehicle Using Disturbance Rejection and Continuous State Damper Controllers. J. Vib. Eng. Technol. Vol. 7, No.2, pp. 117–129 (2019). https://doi.org/10.1007/s42417-019-00088-2

Sharma, S.K., Sharma, R.C., An Investigation of a Locomotive Structural Crashworthiness Using Finite Element Simulation. SAE Int. J. Commer. Veh. Vol. 11, No. 4, pp. 235–244 (2018)., https://doi.org/10.4271/02-11-04-0019

Sharma, S.K., Sharma, R.C., Pothole Detection and Warning System for Indian Roads. In: Advances in Interdisciplinary Engineering Lecture Notes in Mechanical Engineering. Springer, Singapore pp. 511–519 (2019).

Sinha, A.K., Sengupta, A., Gandhi, H., Bansal, P., Agarwal, K.M., Sharma, S.K., Sharma, R.C., Sharma, S.K.: Performance Enhancement of an All-Terrain Vehicle by Optimizing Steering, Powertrain and Brakes. In: Advances in Engineering Design, Lecture Notes in Mechanical Engineering. Springer, Singapore, pp. 207–215 (2019).

Wang, W. Rakheja, S. and Boileau, Paul-Émile,"Effect of back support condition on seat to head transmissibilities of seated occupants under vertical vibration," Journal of Low Frequency Noise Vibration and Active Control, Vol. 25, No. 4, pp. 239-259(2006).

Wickens, A.H., "Fundamentals of rail vehicle dynamics," Swets & Zeitlinger publishers, Netherlands (2003).

Zakeri, J-A. and Ghorbani, V., "Investigation on dynamic behavior of railway track in transition zone," Journal of Mechanical Science and Technology, Vol. 25, No. 2, pp. 287-292(2011).

Zhai, W.M., Cai, C.B. and Guo, S.Z., "Coupling model of vertical and lateral vehicle/track interactions," Vehicle System Dynamics, Vol. 26, No. 1, pp. 61–79(1996).

Zhai, W.M., Wang K . and Cai, C., "Fundamentals of vehicle-track coupled dynamics," Vehicle System Dynamics, Vol. 47, No. 11, pp. 1349–1376(2009).

Zheng J., Matamoros-Sanchez, A., Zolotas, A., Goodall, R., and Smith, M., "Passive suspensions for ride quality improvement of two-axle railway vehicles," Proceedings of the Institution of Mechanical Engineers, Part F: Journal of Rail and Rapid Transit, Vol. 229, No., 3, pp. 315–329(2015).

Zhou, J., Goodall, R., Ren, L. and Zhang, H., "Influences of car body vertical flexibility on ride quality of passenger railway vehicles," Proceedings of the Institution of Mechanical Engineers, Part F: Journal of Rail and Rapid Transit, Vol. 223, No. 5, pp. 461-471(2009).

NOMENCLATURE

A_r Rail cross-sectional area (m^2)

$c_i^{x,z}$ Longitudinal and vertical damping coefficient respectively of body segments (*i = b, d and e*; *b* = upper torso, *d* = pelvic and *e* = upper leg) (N-sec/m)

$c_{ij}^{x,z}$ Longitudinal and vertical damping coefficient respectively between considered body segments (*i, j = a, b, c, d and e*; *a* = head & neck, *b* = upper torso, *c* = viscera, *d* = pelvic and *e* = upper leg) (N-sec/m)

c_{ij}^{z} Vertical damping coefficient between considered rigid bodies of vehicle (*i, j = 1, 2, 3, 4, 5 and 6;* 1= Seat back support, 2= seat, 3=carbody, 4=bolster, 5= bogie frame, 6=wheelaxle) (In Fig. 2 c_{34}^{z} is ½ part, c_{45}^{z} is ½ part, c_{56}^{z} is ¼ part) (MN-sec/m)

$c_{p}^{z,y}$ Rail pad damping coefficient in vertical and lateral directions respectively (MN-sec/m)

$c_{s}^{z,y}$ Ballast damping coefficient in vertical and lateral directions respectively (MN-sec/m)

$I_{i}^{x,y,z}$ Roll, pitch and yaw mass moment of inertia respectively of considered rigid bodies of vehicle (*i, j = 1, 2, 3, 4, 5 and 6)* (kg-m^2)

I_r Rail moment of inertia (m^4)

$k_{i}^{x,z}$ Longitudinal and vertical stiffness respectively of body segments (*i = b, d and e)* (kN/m)

$k_{ij}^{x,z}$ Longitudinal and vertical stiffness respectively between considered body segments (*i, j = a, b, c, d and e)* (kN/m)

k_{ij}^{z} Vertical stiffness between considered rigid bodies of vehicle (*i, j = 1, 2, 3, 4, 5 and 6).*(In Fig. 2 k_{34}^{z} is ½ part, k_{45}^{z} is ¼ part, k_{56}^{z} is ¼ part) (MN/m)

$k_{p}^{z,y}$ Rail pad stiffness in vertical and lateral direction respectively (MN/m)

$k_{s}^{z,y}$ Ballast stiffness in vertical and lateral direction respectively (MN/m)

m_i Mass of human body parts *(i = a, b, c, d & e)* (kg)

m_j Vehicle rigid body mass (*j =1, 2, 3, 4, 5 and 6*) (kg)

$m_{r,s}$ Rail mass (half) and sleeper mass (half) per unit length respectively (kg)

x_{ij} Horizontal distance between considered rigid bodies mass centre of vehicle (*i, j = 1, 2, 3, 4, 5 and 6)* (m)

z_{ij} Vertical distance between considered rigid bodies mass centre of vehicle (*i, j = 1, 2, 3, 4, 5 and 6)* (m).